Reinvestigation of the magnetic behavior of O3–LiCoO2

Alla Artemenko, Michel Ménétrier, Michaël Pollet, Claude Delmas

Reinvestigation of the magnetic behavior of O3−$LiCoO_2$

Alla Artemenko,[a] Michel Ménétrier, Michaël Pollet, and Claude Delmas
ICMCB, CNRS, Université Bordeaux 1, 87 Av. du Dr. A. Schweitzer, 33608 Pessac Cedex, France

(Received 6 April 2009; accepted 19 August 2009; published online 28 September 2009)

Stoichiometric high temperature $LiCoO_2$ obtained by long annealing in oxygen was characterized by electron spin resonance and magnetization measurements. Both methods allow identifying unambiguously not only the presence of traces of cobalt oxides in the material but also paramagnetic defects in lithium cobaltite itself. We report on the presence of surface Li^+-O^- centers in pure $LiCoO_2$, which has not been observed before in this material, and on the presence of Co^{2+} related centers in argon- and subsequent oxygen-annealed samples. © *2009 American Institute of Physics*. [doi:10.1063/1.3226700]

I. INTRODUCTION

Most of the Li-ion batteries for mobile application are still based on a $LiCoO_2$ positive electrode.[1] The exceptional qualities of this material have pushed it right on the market, and this fast success explains why so many studies are still nowadays made on this material to better understand it. In particular, its electronic structure was studied in detail,[2,3] and intensive work was also devoted to the study of its behavior with lithium deintercalation and improvements of its electrochemical properties with doping or substitution.[4–6]

Some of us very recently confirmed that the stoichiometry of (high temperature) $LiCoO_2$ is not a straightforward matter, suggesting that a long annealing under oxygen is required to get rid of a very small amount of excess Li that tends to be accommodated for as $Li_{1+d}Co_{1-d}O_{2-d}$, as soon as the starting Li/Co ratio exceeds 1, be it very slightly. The "really" stoichiometric compound thus obtained was shown to contain only low spin (LS) Co^{3+} ions, based on ^{7}Li NMR relaxation time and magnetization data (at 1 T).[7] However, such very stoichiometric $LiCoO_2$ was also shown to exhibit an antiferromagnetic order below about 30 K using muon spin relaxation experiments, this involving 10% of the volume of the compound;[8,9] the reason for this magnetic behavior is not fully understood yet.

In this context, this paper reports a characterization of such stoichiometric $LiCoO_2$ using electron spin resonance (ESR), the most sensitive technique to the presence of electron spins. ESR has already been extensively used, in particular, by Stoyanova *et al.* in $LiCoO_2$-related compounds, mostly based on the analysis of the signals due to impurity cations (Ni^{3+}) or dopants (Fe^{3+}), from which information on the local structure around the site of the dopant was derived (see, for instance, Ref. 10). Having in mind that a likely source of electron spins might possibly relate to oxygen vacancies and/or to minor impurity phases, we have also investigated samples that were thermally treated in Ar and then in O_2. As a complement to the ESR, we have also studied the magnetic behavior of these samples using a low applied field, which should be more sensitive to the presence of magnetic impurity traces than the earlier ones carried out at 1 T, the structure was investigated by x-ray diffraction (XRD) and the microstructure using scanning electron microscopy (SEM).

II. EXPERIMENTAL

Stoichiometric high temperature $LiCoO_2$ was prepared according to Ref. 7: The Co_3O_4 precursor was prepared by thermal decomposition of $Co(NO_3)_2-6H_2O$ (Sigma-Aldrich ACS reagent, containing less than 10 mg/kg of Fe, Ni, or Cu and less than 20 mg/kg of Mn); it was reacted under oxygen flow with Li_2CO_3 (Alpha Aesar) mixed in stoichiometric amounts, first for 12 h at 600 °C, then, after regrinding at 900 °C for 15 days. This sample will be hereafter named "as synthesized."

This $LiCoO_2$ sample was annealed under Ar at 900 °C for 24 h, and fast cooled in the Ar stream yielding the "Ar-annealed" $LiCoO_2$ sample.

The Ar-annealed compound was in turn annealed under oxygen at 900 °C for 0.5, 5, and 12 h and fast cooled in the oxygen stream, yielding three "O_2-annealed" $LiCoO_2$ samples. Note that, although this is not indicated in their denomination, these samples have also undergone an Ar annealing prior to the O_2 annealing.

XRD patterns were recorded with a PANalytical X'Pert Pro powder diffractometer in the Bragg–Brentano geometry, using cobalt $K\alpha$ radiation. Data collection was made in the 10°–120° 2θ range with a 0.0167° step, using an X'Celerator detector [linear position sensitive detector (PSD) covering 2.122 mm]. Variable temperature XRD patterns were collected using a PANalytical X'pert MPD diffractometer with theta-theta Bragg–Brentano geometry, using the copper $K\alpha$ radiation. An Oxford Instruments He cryostat was used to cool the copper block to which the sample holder is attached (RT to 6 K), in a 10^{-7} mbar chamber.

SEM pictures were recorded with a Hitachi S4500 field emission microscope.

The magnetization of each sample, initial and after annealing, was measured using a Quantum Design magnetic property measurement system within a range from 5 to 320

[a]Author to whom correspondence should be addressed. Electronic mail: alla.artemenko@mail.ru. On leave from IPMS, Institute for Problems of Material Science, Ukrainian Academy of Sciences, 3 Krjijanovsky Str., 03142 Kiev, Ukraine.

TABLE I. Cell parameters' evolution of as-synthesized $LiCoO_2$ in the range 20–293 K (space group $R\bar{3}m$) [profile matching using FULLPROF (Ref. 11)].

Temperature (K)	A (Å)	C (Å)
20	2.8115(1)	14.0164(8)
45	2.8117(6)	14.018(4)
80	2.8119(6)	14.020(4)
293	2.8149(6)	14.048(5)

K both in field-cooled (FC) and zero-field-cooled (ZFC) regimes using an applied field of 1000 G (0.1 T). In addition, measurements versus magnetic field were carried out at several temperatures from 5 to 250 K.

ESR measurements were performed at 9.45 GHz with a Bruker spectrometer in the temperature range 4–300 K using an Oxford Instruments ESR 9 He cryostat. To perform both quantitative and qualitative analyses the same amount (0.05 g) of powder of $LiCoO_2$ samples has been used in the cavity for ESR experiments, while ten times less amount was used in the case of Co_3O_4.

III. EXPERIMENTAL RESULTS

A. XRD

All the samples exhibit the XRD pattern of O3–$LiCoO_2$ (R-3m space group) with no detectable impurity. XRD measurements were also performed for the as-synthesized $LiCoO_2$ in the temperature range 20–293 K, i.e., at temperatures where a magnetic phenomenon had been observed by muon SR,[8,9] and only an increase in the cell parameters with temperature was observed (Table I).

B. SEM

SEM results obtained for the as-synthesized $LiCoO_2$ are shown in Fig. 1. The larger magnification picture shows grains exhibiting steps at their borders, in good agreement with surface energy calculations.[12] In addition, some well separated nanosized particles (with dimensions ranging from 5 to 50 nm) are concentrated nearby coarse surfaces such as uneven grain surface or along the edges of the steps. The surface density of these nanosized particles determined from Fig. 1 is close to 0.1%; considering both their distribution

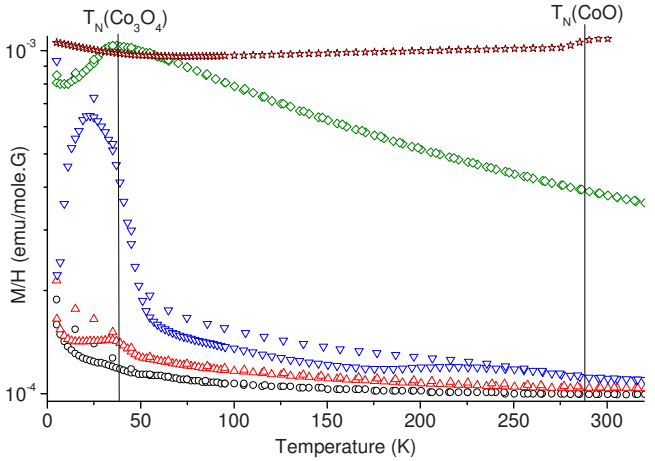

FIG. 2. (Color online) Molar magnetization data vs temperature in FC and ZFC regimes using an applied field of 1000 G for the as-synthesized (○), Ar-annealed (△), and 12 h O_2-annealed (▽) samples. Data measured in the same condition for Co_3O_4 (◇) (this work) and data for CoO (☆) taken from Ref. 13 are also shown; both sets are scaled to match the figure. The vertical lines point the antiferromagnetic-paramagnetic transition temperature for Co_3O_4 and CoO.

(only on the surface of the $LiCoO_2$ particles) and the apparent volume of the $LiCoO_2$ particles, their volume density can be estimated less than 0.1%.

C. Magnetization results

The magnetization data of the as-synthesized sample and after annealing in Ar and O_2 are shown in Fig. 2. All samples exhibit a low positive signal at RT. It (slightly) increases with decreasing temperature up to an inflection point (as-synthesized sample) or a maximum (annealed samples) nearby 30 K. In addition, a small upturn is visible in ZFC curves below 15 K. The ZFC and FC curves separate around 40 K for the as-synthesized sample while the separation occurs at ~40 and 290 K for the annealed samples. The high temperature separation is clearer in the case of the O_2-annealed samples.

Measurements versus magnetic field carried out at 5 K for the as-synthesized sample, the argon-annealed and the argon—then 5 and 12 h oxygen-annealed samples—are shown in Fig. 3. The as-synthesized and argon-annealed samples display a quite similar and nearly linear behavior of the magnetization versus the magnetic field, and only sub-

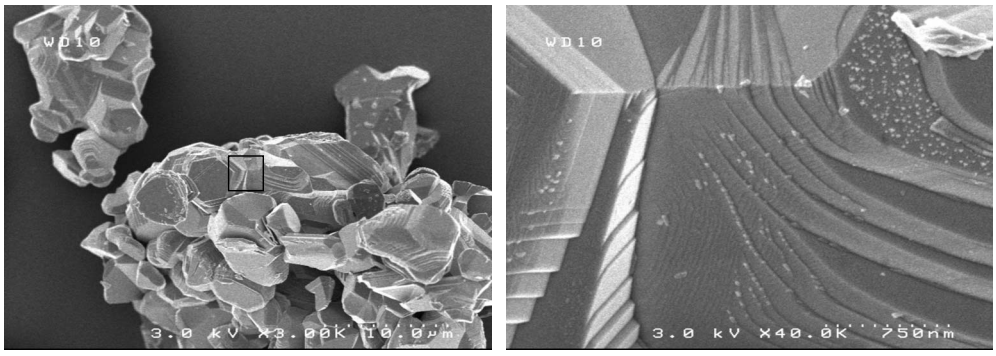

FIG. 1. SEM data for the as-synthesized sample.

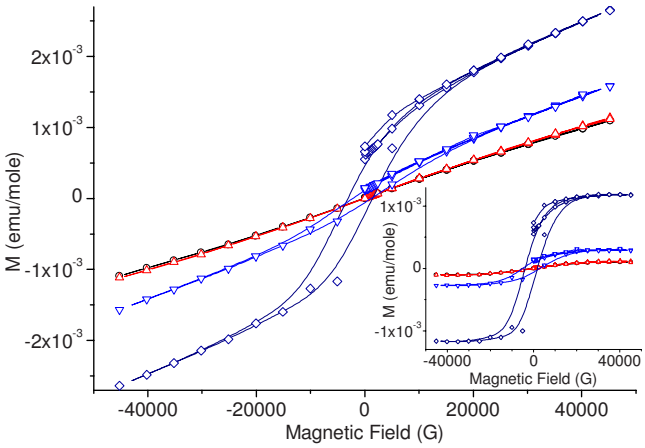

FIG. 3. (Color online) Molar magnetization data vs magnetic field at 5 K for the as-synthesized (○), Ar-annealed (△), 5 h O_2-annealed (◇), and 12 h O_2-annealed (▽) samples. Inset: same data with the linear contribution subtracted (n_0: amount of product used for the analysis assuming a zero impurity rate).

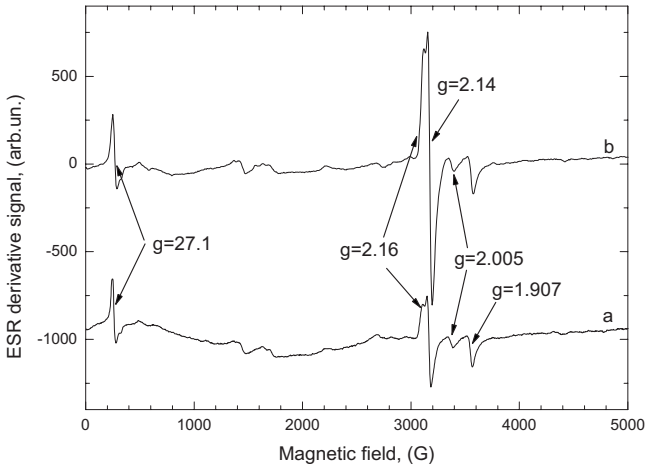

FIG. 5. ESR spectra recorded at 4.2 K for (a) as-synthesized $LiCoO_2$ and (b) Ar-annealed sample.

tracting the linear contribution allows seeing a tiny nonlinear behavior. On the other hand, the oxygen-annealed samples have a pronounced hysteretic behavior.

The inset in Fig. 4 shows for the argon then 5 h oxygen-annealed sample some of the magnetization data recorded versus the magnetic field at several temperatures (linear contribution subtracted). The hysteretic behavior is visible up to nearly 75 K and then completely vanishes. These data are plotted versus temperature in Fig. 4 for several magnetic fields evidencing the disappearance of the nonlinear regime around 75 K.

D. ESR of $LiCoO_2$

1. As-synthesized and argon-annealed samples

Figure 5 shows ESR spectra recorded at 4.2 K for the as-synthesized $LiCoO_2$ sample and after annealing in argon.

Similar spectra are observed for both samples at 4.2 K and their temperature evolution is almost the same (see further). The most intense ESR lines have g-factors $g=27.1$, $g=2.16$, $g=2.14$, $g=2.005$, and $g=1.907$. After annealing in Ar, only the lines with g-factors 2.16 and 2.14 change significantly with intensity approximately multiplied by 3. All lines marked in Fig. 5, with the exception of the one at $g=2.16$, are observed up to room temperature (RT) with changes described below.

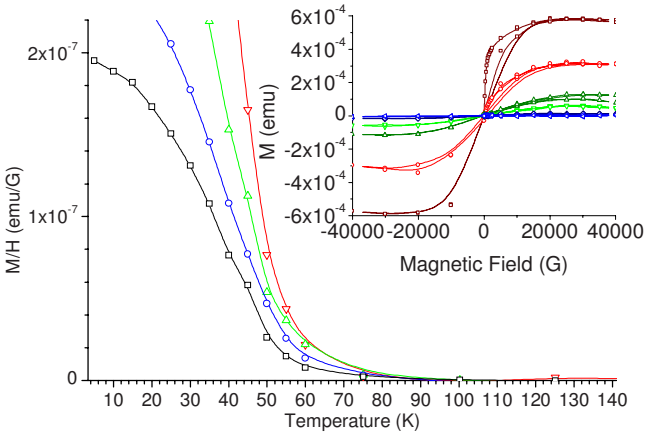

FIG. 4. (Color online) Sample residual magnetization vs temperature determined from the $M(H)$ curves at several magnetic fields for the 5 h oxygen-annealed sample (▽: 1, △: 2, ○: 3, and □: 4 T). Inset: some of the magnetization data vs magnetic field (linear contribution subtracted) for the same sample at several temperature (□: 35, ○: 45, △: 55, ▽: 60, ◇: 75, and ◁: 100 K).

Above 120 K the position of the lines with g-factors $g=27.1$, $g=2.005$, and $g=1.907$ changes: (i) The distance between the two furthest lines begins to decrease and at RT the corresponding g-factors are 19.58 and 1.924; i.e., the shift is about 130 G. (ii) The line at $g=2.005$ slightly shifts upward to $g=2.01$ at RT (~15 G). Moreover, with increasing temperature the line width trend for these resonances changes from increasing below 38 K to nearly constant up to 90 K and finally increasing again up to RT by a factor ~1.5–2. The behavior of the $g=2.14$ line is slightly different with a small increase in the line width up to 20 K then a plateau up to 90 K and finally decreases up to RT.

A closer look in Fig. 5 at the $g=2.14$ line evidences a doublet at 4.2 K. Additional experiments performed in the narrow magnetic field region 3000–3300 G allowed separating the lines. An example of separation of the lines in the spectrum recorded at 4.2 K for the as-synthesized sample is shown in Fig. 6, evidencing a perfect agreement between experimental data and the simulation with five lines.

A similar treatment was carried out up to 20 K (not shown) when the $g=2.16$ line disappears and the ESR spectrum becomes symmetric. The first observation is that five components (dashed lines 1–5 in Fig. 6) are required to reproduce the experimental sets. A second one is the complexity of the line at $g=2.16$, which can actually be described as the sum of four lines (as depicted with line 6 in Fig. 6). These four lines exhibit the same temperature dependence, decreasing identically up to disappearance at 20 K. The fast disappearance of this set of lines together with its very low and narrow existence range in temperature allows assuming that it should originate either from (i) a paramagnetic defect with a very short relaxation time or (ii) a center localized

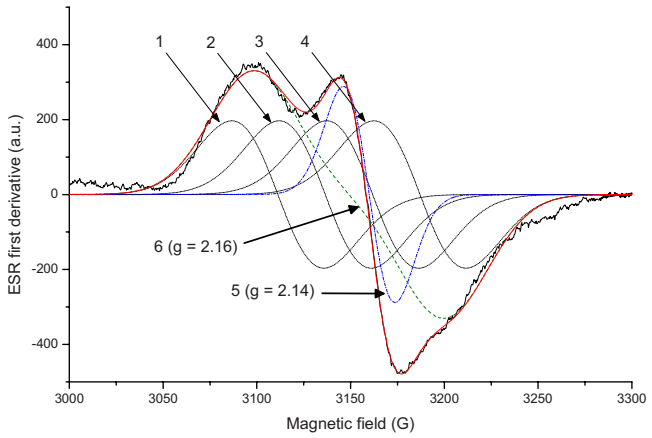

FIG. 6. (Color online) Experimental data at 4.2 K for as-synthesized $LiCoO_2$ (black solid line) and results of the decomposition (black dotted lines 1–4 and blue dotted-dashed line 5); dashed line 6—sum of lines 1–4.

nearby the surface of the sample and having a low activation energy or (iii) a center with a very shallow level in the band gap of lithium cobaltite.

Furthermore, the fact that the *g*-value of this set is larger than the free electron one but anyway quite close suggests an origin in a hole-center type.

It is known that the integral intensities of the ESR lines originating from the same paramagnetic defect display identical behavior versus temperature.[14] The temperature dependence of the integral intensities of the most intense ESR lines for the as-synthesized $LiCoO_2$ sample is depicted in Fig. 7.

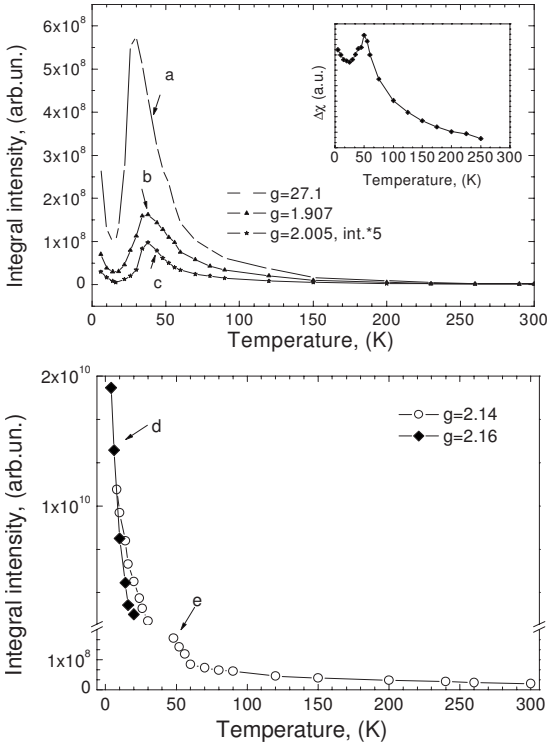

FIG. 7. Integral intensities' temperature dependence of the ESR spectra observed for as-synthesized $LiCoO_2$: (a) $g=27.1$, (b) $g=1.907$, (c) $g=2.005$ (top), (d) $g=2.16$, and (e) $g=2.14$ (bottom). The inset in the top figure shows, for the 5 h oxygen-annealed sample, the susceptibility extracted from the linear part of the $M(H)$ curves at several temperatures minus the second order contribution of the Co^{3+} cation in $LiCoO_2$.

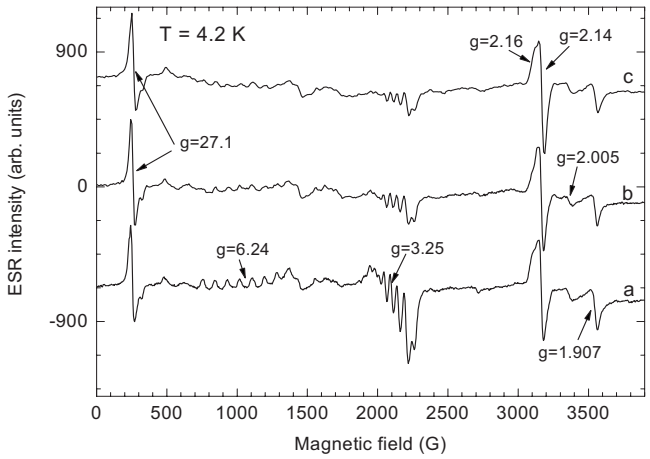

FIG. 8. $LiCoO_2$ after annealing in O_2: (a) 0.5, (b) 5, and (c) 12 h.

Three different paramagnetic centers are evidenced: (i) one leading to the three lines at $g=27.1$, $g=2.005$, and $g=1.907$; (ii) a second one at $g=2.16$; and (iii) a last one at $g=2.14$. The ESR lines of smaller intensity in the magnetic field region 200–2900 G roughly follow the integral intensity temperature dependence observed for the line at $g=2.14$. (The inset in Fig. 7 is discussed in Sec. IV).

2. Argon- then oxygen-annealed samples

ESR spectra at 4.2 K for the oxygen-annealed samples are shown in Fig. 8. Additional resonances appear in these spectra while the intensity of all ESR lines previously described is decreased: For the lines with *g*-factors 2.16 and 2.14, the intensity is divided by more than 10; for the remaining lines, the intensity is only divided by 1.5; small intensity resonances previously observed in the magnetic field region 900–2900 G are smeared out.

These additional resonances clearly appear in the magnetic field region 500–2400 G at approximately $g=6.24$ and $g=3.25$. The existence of eight hyperfine lines in this spectrum allows identifying it unambiguously as originating from cobalt ion (^{59}Co), which has a nuclear spin 7/2 of 100% natural abundance. Moreover, the presence of several of these hyperfine octets signs a symmetry lower than O_h. Furthermore, the appearance of these additional resonances only after the second annealing in oxygen (this signal is not present for the as-synthesized nor for the simply argon-annealed sample) indicates an oxygen related center. It can be noticed that increasing the oxygen annealing time leads to a decrease in the ESR intensity of this spectrum, which suggests a center located near the surface. Besides, its integral intensity decreases with the measurement temperature for all samples and completely vanishes above 50 K (not shown).

The RT spectra of these oxygen-annealed samples are very similar to the one described for the previous samples; only two broad lines appear, one in low magnetic field region ($g=4.35$) with line width ~1500 G and a second one in higher magnetic field at $g=2.24$ and line width ~900 G.

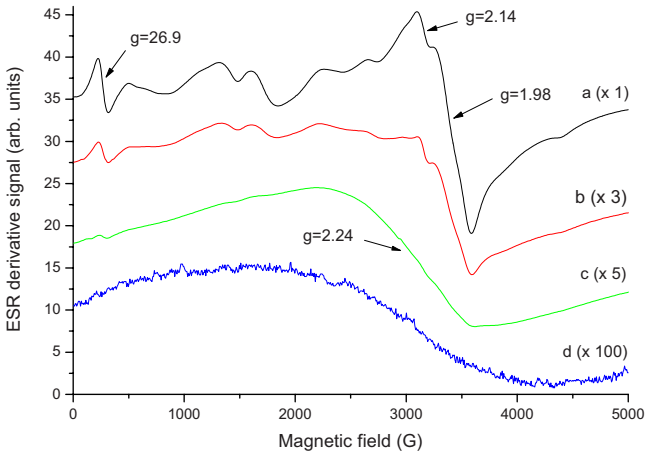

FIG. 9. (Color online) ESR spectra of Co_3O_4 recorded at several temperatures. From top to bottom: (a) 4.2 K, (b) 25 K, (c) 45 K, and (d) RT. (The numbers in parentheses following the spectra labels are scale factors.)

3. Co_3O_4

Additional ESR studies of powder Co_3O_4 sample (the starting material used for preparing the $LiCoO_2$ samples) have been performed to separate between the signals originating from lithium cobaltite and unreacted precursors, if any. The spectrum recorded on Co_3O_4 powder sample at 4 K is shown in Fig. 9; the signal being quite strong, only 0.01 g of powder has been used.

The spectrum is very close to the one observed for the as-synthesized and Ar-annealed $LiCoO_2$ samples but the lines are more intense and broader. In addition a broad line in the magnetic field region 2000–5000 G prevents any further line separation in this region even though some resonances can be observed. Above 35 K, an even broader and more intense line (>4000 G) at $g=2.24$ appears; it broadens and decreases in intensity with temperature increasing. It covers all other lines except one in low magnetic field at $g=26.9$. This last resonance is not anymore visible at RT both because of its shift to high magnetic field and because of the broadening of the most intense lines and their overlap.

IV. DISCUSSION

The structure of stoichiometric high temperature $LiCoO_2$ (Ref. 15) is of rocksalt type with an ordering of the lithium and cobalt ions in the [111] direction leading to alternate planes of lithium and cobalt atoms. This ordering leads to a trigonal distortion of the oxygen octahedron surrounding the cobalt, which is compressed and leaves Co^{3+} in a D_{3d} symmetry; conversely, the LiO_6 octahedron is elongated. Theoretical calculations have shown that the Co^{3+} ion with its $6d$ electrons is the most favorable case for stabilizing a LS state ($S=0$) in this oxygen surrounding.[16] This is confirmed experimentally since most of Co^{3+} complexes contain no unpaired electron spins and are diamagnetic. Very few examples are available in literature showing unambiguously the existence for this ion of higher spin states; this situation is always related to highly distorted environments.[17,18] The ground state configuration of Co^{3+} is a low lying orbital triplet $t_{2g}^6 e_g'^0$ or, accounting for the distortion that further splits the triplet in a low lying doublet, and an upper singlet $e_g^4 a_{1g}^2 e_g'^0$.[19,20] With such a ground state, the t_{2g} shell is completely filled and only a slight temperature dependent paramagnetism is expected. Note, however, that the orbital moment might only partly be quenched and that it can still play a significant role in the magnetic properties at (very) low temperature. Over all, it remains that, for a "pure" stoichiometric $LiCoO_2$, no intrinsic paramagnetic defects related to Co^{3+} ions are expected. This is obviously in contradiction with the results of the present study, which clearly show both with magnetic and EPR measurements that some paramagnetic centers are present in the samples (Figs. 2–8).

A qualitative analysis of the EPR results shown in Fig. 5 (as-synthesized and Ar-annealed samples), Fig. 8 (Ar then O_2-annealed samples), and Fig. 9 (Co_3O_4) shows that a number of the main resonance lines in our materials are identical to the ones of Co_3O_4. In addition, the integral intensities' temperature dependence of these lines is very similar to the one obtained from magnetic measurements [Fig. 2; inset of Fig. 7 (top)]. Since the integral intensity is proportional to the static magnetic susceptibility of the ions responsible for the signal,[14] this evidences their unique origin. As shown in Fig. 2, the anomalies in the magnetization curves around 40 and 290 K are characteristic of the antiferromagnetic ordering in the cobalt oxides Co_3O_4 and CoO.[13] This indicates that all the samples, including the most carefully prepared one (as synthesized), contain cobalt oxides as secondary/impurity phases. The additional annealing treatments only enhance their signal, and we ascribe this to the partial decomposition of the sample into cobalt oxides. Keeping in mind that Co_3O_4 has a normal spinel structure where Co^{2+} ions are in tetrahedral coordination and Co^{3+} ions are in octahedral coordination with, respectively, $S=3/2$ and $S=0$,[21,22] it appears obvious that the spectra observed in Fig. 9 and the corresponding lines in Figs. 5, 7, and 8 originate from Co^{2+} in tetrahedral symmetry. It should be noticed that in spite of careful experiments and analysis, no trace of these cobalt oxides could be observed using XRD, and that only EPR experiments and magnetization measurements could reveal their presence. This points out that laboratory's XRDs are not sufficiently accurate to discard the presence of impurities in such low amount, even though their concentration is sufficient to determine the magnetic behavior of the samples. The amount of impurities in the as-synthesized sample has been estimated from the temperature variation of the magnetization data, assuming the only presence of Co_3O_4 and a temperature independent paramagnetism (TIP) term for $LiCoO_2$ due to LS state Co^{III}: Co_3O_4: $LiCoO_2$=0.062% (molar ratio) and TIP=153×10^{-6} emu/mole. The Co_3O_4 amount estimated from this assumption is in line with the SEM observation (Fig. 1). The TIP is due to a second order Zeeman contribution related to the splitting of the d orbitals by the crystal field. For an $^1A_{1g}$ ground state, and assuming an octahedral symmetry for the cobalt (the D_{3d} distortion is neglected in a first approximation), the TIP is given by $8N\beta^2/10Dq$,[23] leading to a t_{2g}-e_g splitting of 1.7 eV for $LiCoO_2$, in good agreement with our optical spectra (not shown), and with the insulating behavior of $LiCoO_2$. A similar treatment (including CoO in the calculation) for the annealed samples keeps the TIP unchanged while the total

amount of cobalt oxides increases from 0.12% (0.11% Co_3O_4) in the argon-annealed sample to nearly 0.5% (0.3% Co_3O_4) and 1% (0.2% Co_3O_4) in the 5 and 12 h oxygen-annealed samples, respectively. The small decrease in the Co_3O_4 amount with the annealing time in oxygen is also visible from ESR measurements (Fig. 8) with the slight decrease in the integral intensity of the lines attributed to Co_3O_4.

Even though the resonance lines observed for Co_3O_4 are also found in $LiCoO_2$ spectra, all the line widths in the lithium cobaltite are narrower than the ones of the cobalt oxide; in both cases anyway, the broadening makes it impossible to resolve the hyperfine structure of Co nuclei in Co_3O_4. Several reasons (nonexclusive) can be proposed for this broadening: (i) The samples are powders and the signal is averaged over all the orientations; (ii) the centers are highly concentrated in the structure (one Co^{2+} per f.u.); (iii) the spin-spin exchange interaction between neighbors; and (iv) the dipolar interactions with neighboring electronic and nuclear spins can be large since high fields are expected in such structure (the magnetic field produced by an electron at a distance of 4 Å is approximately 600 G; in addition, in materials containing transition metals, it is possible to have an on-site magnetic field variation as high as 1000 G throughout the crystal). The narrowing of the lines in the case of Co_3O_4 observed in $LiCoO_2$ might be due to the microstructure: The cobalt oxide particles are nanosized and are well separated as shown in SEM pictures (Fig. 1). This decreases the effects previously cited (i–iv). Moreover, the particles' size is 5–50 nm, and one can expect a significant contribution to the ESR and magnetization of the centers nearby the surface. Note that in the nanosize case, the contribution of the surface centers can be of the same order of magnitude than the bulk's ones like it was shown for ferroelectric nanomaterials.[24] In ESR spectra this contribution can either lead to (i) a line broadening, (ii) lines' asymmetry, and (iii) the appearance of an additional spectrum due to uncompensated spins or lowering in symmetry at the surface of the nanoparticles.[25] It should be noticed that the upturn in magnetization data at low temperature also seems to be characteristic of nanometric Co_3O_4; it has been attributed to the coexistence of frustrated shell spins and antiferromagnetic core spins.[22,26] One can notice that a hysteretic behavior was observed in Co_3O_4 nanoparticles[27–29] and was attributed to uncompensated surface spins; however, contrary to our results (Figs 3 and 4), this behavior was vanishing above the Néel temperature.[27,29]

The annealing in oxygen following the Ar annealing leads to the appearance of an additional spectrum (Fig. 8). The strong features in the magnetic field region 500–2400 G correspond to the hyperfine structure associated with high-spin Co^{2+} in a distorted octahedron; details of this assignment are discussed elsewhere.[30] In the general case, such spectrum can be simulated assuming a simple axial distortion and using the following Hamiltonian:[14]

$$H = g_{\|}\beta H_z \bar{S}_z + g_{\perp}\beta(H_x \bar{S}_x + H_y \bar{S}_y) + A_{\|}\bar{S}_z I_z + A_{\perp}(\bar{S}_x I_x + \bar{S}_y I_y),$$

where β is the Bohr magneton, g is the electron gyromagnetic factor (in the case of Co^{2+} we have considered the effective g tensor, consisting from electron spin and the contribution from orbital moment), $\bar{S}$ is effective electron spin for lowest doublet describing two-level system, I is the nuclear spin, and A is the hyperfine interaction tensor. Using an effective electron spin $\bar{S}=1/2$ and nuclear spin $I=7/2$, the adjusted parameters are $g_{\|}=6.376(2)$, $10^4|A_{\|}|=232(4)$ cm^{-1}, $g_{\perp}=3.268(2)$, and $10^4|A_{\perp}|=25(2)$ cm^{-1}. Note that the average value of $g=4.304$ is close to the one predicted by crystal field theory for the Co^{2+} ion in octahedral crystalline field. The fact that the hyperfine structure is present on either sides of the antiferromagnetic ordering of Co_3O_4 discards an origin of the signal in cobalt from the Co_3O_4 secondary phase. Indeed, above T_N, the Co_3O_4 particles' core centers are in a paramagnetic state and they should strongly interact with the shell centers and broaden the lines, making impossible to resolve the hyperfine structures; however, they are still visible up to at least 50 K and only a decreasing in their intensity was observed. The magnetic data also discard an origin in Co_3O_4: The magnetic hysteresis associated with these additional resonances is visible up to nearly 75 K, a temperature much higher than the Neel temperature of Co_3O_4 that can moreover be lowered in the case of nanoparticles;[26] this hysteresis denotes a long range ordering with a parallel coupling of the spins and either a ferro- or ferrimagnetic behavior and even though a hysteretic behavior has already been observed in nano-Co_3O_4,[27,28] it was disappearing above T_N.[29] Furthermore, the fact that these additional resonances' intensity is decreasing with the annealing time while, as shown from magnetization data, the CoO content is increasing discards also an origin of the signal of cobalt from the CoO secondary phase. The hysteretic behavior observed for the O_2-annealed samples, as well as the main Co^{2+} ESR signal (Fig. 8), might therefore be due to defects related to $LiCoO_2$. We ascribe this spectrum to the creation of Co^{2+} surface centers in $LiCoO_2$: The as-synthesized sample has undergone a long thermal treatment (15 days), and the number of defaults at the surface of the sample should be minimized; the argon annealing was also quite long (1 day) and one can still expect for a homogenous sample; on the other hand, the annealing in oxygen was shorter and was ranging from only 30 min to 12 h, which seems favorable to the appearance of a perturbed shell; this assumption is further reinforced with the observation, with increasing annealing time, of the decreasing of the ESR lines' intensity (Fig. 8) and of the magnetization (Fig. 3).

The line at $g=2.14$ exhibits the same T-dependence of the integral intensity as the small intensity lines in the magnetic field region 200–2900 G evidencing a common origin for these resonances. These latter lines are also visible in Co_3O_4 powder (Fig. 9), at the same position but with an enhanced intensity; thus the line at $g=2.14$ can be attributed to paramagnetic defects in Co_3O_4.

The line at $g=2.16$ was not reported yet in $LiCoO_2$ (as-

synthesized and annealed samples). Its existence both at very low temperature and in a narrow temperature range is due to a short relaxation time. The four lines used to separate the spectrum (equidistant lines 1–4 in Fig. 6) have fixed positions and all decrease in intensity when the temperature increases. This indicates that these lines result from a hyperfine interaction ($10^4 \times |A_{iso}| \sim 23$ cm^{-1}) with an associated paramagnetic defect of nuclear spin $I=3/2$, and two ions can here be considered: lithium and nickel (as classical impurity of cobalt). ^{7}Li isotope has a 92.5% natural abundance, a nuclear spin $I=3/2$, and a nuclear g-factor $g_N=2.17$; ^{6}Li isotope has a 7.5% natural abundance, a nuclear spin $I=1$, and a nuclear g-factor $g_N=0.82$. ^{61}Ni isotope has only 1.13% natural abundance, a nuclear spin $I=3/2$, and a nuclear g-factor $g_N=-0.5$; on the other hand, the remaining nickel stable isotopes have $I=0$ nuclear spin that would lead to an intense line associated with the hyperfine quartet. Such a line is not observed, discarding the nickel origin of the quartet as expected from the purity of the Co source used for preparing the compounds. The observed resonance thus originates from lithium with defect in its nearest neighborhood. Furthermore, this ESR has a large magnitude while the characteristic magnetic signatures of the cobalt oxides, in particular, the transition temperatures, are unperturbed; this discards an origin in some possible lithium impurities in the traces of cobalt oxides and implies that this resonance originates from $LiCoO_2$ itself. Indeed, if the former were to contain significant amounts of Li, as would be implied by the magnitude of the EPR signal, their magnetic signature would significantly differ from those of Co_3O_4 and/or CoO. We suggest a paramagnetic center of Li^+-O^-. The O^- related centers were studied in some perovskites,[31] and calculations have shown that they are preferably localized near the surface. Here also, the Li^+-O^- paramagnetic centers are more likely to be localized near the surface since all the lines related to this center resonances are broader than those expected from bulk's centers. The broadening of the EPR lines is due to the distribution of the resonance fields because of the numerous vibronic states nearby surface. The decreasing magnitude of this line with the O_2 annealing further strengthens these assumptions of an oxygen related center and a surface localization; the nonlinearity of the integral intensity depending on the annealing time can be due to the competition between several processes occurring simultaneously in the samples, for example, electron trapping at oxygen ion (Li^+-O^-/Li^+-O^{2-} creation) and decomposition of $LiCoO_2$.

V. CONCLUSIONS

Several methods have been used to characterize the magnetic behavior of stoichiometric $LiCoO_2$. A combined analysis of the data in a wide range of temperature allows straightening out several important points: (i) The pure stoichiometric $LiCoO_2$ displays a purely TIP with no evidence for any kind of ordering; (ii) neither oxygen vacancies nor Co^{4+} associated centers were observed and they appear unlikely in the stoichiometric compound; (iii) in spite of high care in the sample preparation, traces of secondary phases look unavoidable; (iv) some nanosized particles at the surface of the sample were identified as cobalt oxides based that cause the main contribution to the magnetic properties and the ESR signature of the $LiCoO_2$ material at low temperature; we did not observe any intrinsic magnetic ordering in the $LiCoO_2$ phase like the one hypothesized by Sugiyama based on muon SR; (v) surface Li^+-O^- centers described in this article were not reported yet in this material; (vi) $LiCoO_2$ is unstable above 800 °C in argon and decomposes with Li_2O volatilization and further in oxygen if its surface is altered; (vii) the two step annealing (Ar then O_2) also favors the appearance of Co^{2+} surface defects as evidenced with the presence of an additional spectrum and a residual magnetization.

VI. ADDENDUM

During the revision procedure of this paper, an article on Fe-doped $LiCoO_2$ has been published by Stoyanova *et al.*[32] In this paper, the authors observe an EPR spectrum at 9.2 GHz [Fig. 1(a)] very close to the one observed in our work. They assigned these resonances to Fe^{3+} dopant and resonance at $g=2.14$ to Ni^{3+} impurity in $LiCoO_2$. As discussed in our paper, we ascribe the observed spectrum to the presence of cobalt oxides in the lithium cobaltite samples as a secondary phase based on EPR temperature dependence and magnetization measurements, performed on $LiCoO_2$ and cobalt oxide.

ACKNOWLEDGMENTS

The authors thank Cathy Denage for technical assistance and Eric Lebraud for the variable temperature XRD data collection. A.A. acknowledges the University of Bordeaux 1 for invitation.

[1] K. Mizushima, P. C. Jones, P. J. Wiseman, and J. B. Goodenough, Mater. Res. Bull. **15**, 783 (1980).
[2] J. van Elp, J. L. Wieland, H. Eskes, P. Kuiper, G. A. Sawatzky, F. M. F. de Groot, and T. S. Turner, Phys. Rev. B **44**, 6090 (1991).
[3] M. T. Czyzyk, R. Potze, and G. A. Sawatzky, Phys. Rev. B **46**, 3729 (1992).
[4] M. Ménétrier, I. Saadoune, S. Levasseur, and C. Delmas, J. Mater. Chem. **9**, 1135 (1999).
[5] V. R. Galakhov, V. V. Karelina, D. G. Kellerman, V. S. Gorshkov, N. A. Ovechkina, and M. Neumann, Phys. Solid State **44**, 266 (2002).
[6] F. Gendron, S. Castro-Garcia, E. Popova, S. Ziolkiewicz, F. Soulette, and C. Julien, Solid State Ionics **157**, 125 (2003).
[7] M. Ménétrier, D. Carlier, M. Blangero, and C. Delmas, Electrochem. Solid-State Lett. **11**, A179 (2008).
[8] K. Mukai, Y. Ikedo, H. Nozaki, J. Sugiyama, K. Nishiyama, D. Andreica, A. Amato, P. L. Russo, E. J. Ansaldo, J. H. Brewer, K. H. Chow, K. Ariyoshi, and T. Ohzuku, Phys. Rev. Lett. **99**, 087601 (2007).
[9] K. Mukai, J. Sugiyama, Y. Ikedo, H. Nozaki, K. Shimomura, K. Nishiyama, K. Ariyoshi, and T. Ohzuku, J. Power Sources **174**, 711 (2007).
[10] R. Stoyanova, E. Zhecheva, and J. L. Tirado, J. Phys. Chem. B **108**, 4053 (2004).
[11] J. Rodríguez-Carvajal, Physica B **192**, 55 (1993).
[12] L. Dahéron, H. Martinez, R. Dedryvère, I. Baraille, M. Ménétrier, C. Denage, C. Delmas, and D. Gonbeau, J. Phys. Chem. C **113**, 5843 (2009).
[13] J. R. Singer, Phys. Rev. **104**, 929 (1956).
[14] A. Abragam and B. Bleaney, *Electron Paramagnetic Resonance of Transition Ions* (Clarington, Oxford, 1970).
[15] S. H. J. Orman and P. J. Wiseman, Acta Crystallogr., Sect. C: Cryst. Struct. Commun. **40**, 12 (1984).
[16] M. Pouchard, A. Villesuzanne, and J. P. Doumerc, C. R. Chim. **6**, 135 (2003).
[17] J. P. Doumerc, M. Coutanceau, L. Fournes, J. C. Grenier, M. Pouchard,

and A. Wattiaux, Comptes Rendus de l'Académie des Sciences - Series IIC - Chemistry **2**, 637 (1999).
[18]S. Aasland, H. Fjellvag, and B. Hauback, Solid State Commun. **101**, 187 (1997).
[19]S. Landron and M. B. Lepetit, Phys. Rev. B **74**, 184507 (2006).
[20]M. Pollet, J. P. Doumerc, E. Guilmeau, D. Grebille, J. F. Fagnard, and R. Cloots, J. Appl. Phys. **101**, 083708 (2007).
[21]W. L. Smith and A. D. Hobson, Acta Crystallogr., Sect. B: Struct. Crystallogr. Cryst. Chem. **B29**, 362 (1973).
[22]L. He, C. Chen, N. Wang, W. Zhou, and L. Guo, J. Appl. Phys. **102**, 103911 (2007).
[23]B. N. Figgis, in *Ligand Field Theory and its Applications*, edited by M. A. Hitchman (Wiley-VCH, New York, 1999).
[24]I. P. Bykov, M. D. Glinchuk, V. V. Laguta, A. M. Slipenyuk, L. Soukup, L. Jastrabik, and M. Hrabovsky, Integr. Ferroelectr. **32**, 159 (2001).
[25]A. M. Slipenyuk, I. V. Kondakova, M. D. Glinchuk, and V. V. Laguta, Phys. Status Solidi. C **4**, 1297 (2007).
[26]R. N. Bhowmik, R. Nagarajan, and R. Ranganathan, Phys. Rev. B **69**, 054430 (2004).
[27]Y. Ichiyanagi and S. Yamada, Polyhedron **24**, 2813 (2005).
[28]H. M. Chen, R. S. Liu, H. L. Li, and H. C. Zeng, Angew. Chem., Int. Ed. **45**, 2713 (2006).
[29]Y. Ichiyanagi, Y. Kimishima, and S. Yamada, J. Magn. Magn. Mater. **272-276**, E1245 (2004).
[30]A. P. Abragam and M. H. L. Pryce, Proc. R. Soc. London, Ser. A **206**, 173 (1951).
[31]V. V. Laguta, A. M. Slipenyuk, I. P. Bykov, M. D. Glinchuk, M. Maglione, D. Michau, J. Rosa, and L. Jastrabik, Appl. Phys. Lett. **87**, 022903 (2005).
[32]R. Stoyanova, A.-L. Barra, E. Zhecheva, R. Alcantara, G. Ortiz, and J. L. Tirado, Inorg. Chem. **48**, 4798 (2009).